AN EXPERIMENTAL STUDY OF TRACE AND RARE EARTH ELEMENT (REE) PARTITIONING BETWEEN CAI-TYPE MELTS AND GROSSITE: IMPLICATIONS FOR PROCESSES DURING CAI FORMATION

G. Ustunisik[1], D. S. Ebel[1,2], D. Walker[2,1], [1]Department of Earth and Planetary Sciences, American Museum of Natural History, New York, NY, 10024 (gustunisik@amnh.org) [2]Department of Earth and Environmental Sciences, Lamont Doherty Earth Observatory of Columbia University, Palisades, NY, 10964-8000.

Introduction: Ca-, Al-rich inclusions (CAIs) in chondrite meteorites are the oldest crystalline solids in the solar system. Therefore, the variations of trace element concentrations within individual CAIs can provide crucial information into the nature of processes effective in the primitive solar nebula. Despite most CAIs having complex histories during and after their initial formation [1], high-temperature, Type B (igneous) CAIs [2, 3] offer a unique opportunity to understand the distribution of trace elements in a controlled magmatic system which underwent fractional crystallization from a single starting liquid of a known bulk composition, crystallization sequence [4], and approximately known cooling rate [5, 6].

The mineralogy of Type B CAIs is dominated by refractory oxides and silicates such as spinel, melilite, Al-, Ti-bearing clinopyroxene, and grossite. These minerals are among the first solids predicted to condense from a hot cooling gas of solar composition [3,7] and therefore the trace element abundances and distribution among these minerals can reveal information about the processes of CAI formation including the role of volatilization, fractional condensation, and fractional crystallization. However, the accurate assessment of how Type B CAIs crystallized requires knowledge of the appropriate mineral–melt partition coefficients.

While fairly extensive analytical data exists on trace element partitioning between certain phases (anorthite, clinopyroxene, hibonite, perovskite, and melilite) and CAI type melts, partition coefficients are very sparse for spinels - especially at various oxygen fugacities; and completely missing for rarer phases such as grossite [8]. Furthermore, previous experimental partitioning data is only available for certain trace elements and is limited to phases such as melilite, perovskite, spinel, and diopside [9-12] and to a single bulk liquid composition.

Here, we designed crystallization experiments using various bulk compositions from [13] to determine partitioning of trace and REEs in specific fields of condensation space (Fig. 1) between grossite, melilite and CAI-type liquids. These results will provide systematic constraints on compositional, temperature, and oxygen fugacity dependence of trace and REE partitioning between solids and CAI-type liquids. This abstract reports only on preliminary experiments on the partitioning of trace elements and REEs between grossite and CAI-type liquids.

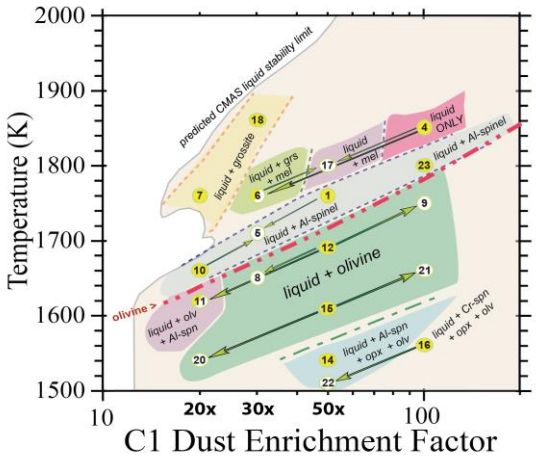

	SiO_2	TiO_2	Al_2O_3	FeO	MgO	CaO	Total
#18	5.09	1.89	59.03	0	0.18	33.81	100

Fig. 1. Experimentally determined phase fields from [13] with the bulk composition of #18. Figure is adapted from predictions in plate 10 of [14].

Experimental Design: Experiments were performed at 5 GPa using the bulk composition of #18 from Fig. 1, doped with La, Ce, Eu, Dy, Ho, Yb, Th, Zr, Hf, Nb, Ta, Sr, and B to determine partitioning between grossite and CMAS-liquid. A high-pressure medium was chosen to retain the desired volatile trace elements abundances in the melt.

Composition #18 was prepared from a mixture of oxides, silicates, and carbonates by homogenization in ethanol in an automated mortar for >1 hour and drying at 175°C under vacuum. Dopant was prepared from high purity oxides of La, Ce, Eu, Dy, Ho, Yb, Zr, Hf, Tb, and Ta; carbonates of Sr and Ba; Th as the mineral thorianite ThO_2; and B as boric acid H_3BO_3. After grinding by hand in an agate mortar with ethanol, dopant powder was decarbonated and denitrified at 1000 °C overnight. Lacking sufficient starting material (#18 [13]) to dilute the trace element dopant mix, we first diluted 1 g of the dopant powder with 9 g of synthetic grossite mix. Then 0.005 g of this grossite + dopant mix was diluted with 0.5 g of composition #18 to produce 50 ppm concentrations of each trace element in the final experiment. The total concentration of all trace and REEs was kept <1000 ppm in order not to disturb the phase equilibria.

High pressure experiments were conducted at Lamont-Doherty Earth Observatory (LDEO) using piston-cylinder apparatus at 1590°C and 5 GPa for 50 hours.

The assembly was a Pb-wrapped $BaCO_3$/MgO pressure medium, graphite furnace, high-density Al_2O_3 sleeve (0.25″), one-hole and solid MgO spacers (0.5″), MgO wafer (1.5 mm), and graphite sample capsules (6 mm length with a 3 mm internal cavity). Experiments were typically pressurized cold then heated in slow steps to 850°C over an hour after which the assembly was left at that temperature, typically overnight to stabilize and close porosity in the pressure media and graphite capsules. After repressurization, temperature was raised in steps of typically 20 min to the run temeperature, repressurized after 20 min, and left to cook for >2 days (50 hours). Quench was accomplished by turning off the power. Cooling to below 400°C typically took approximately 5 seconds.

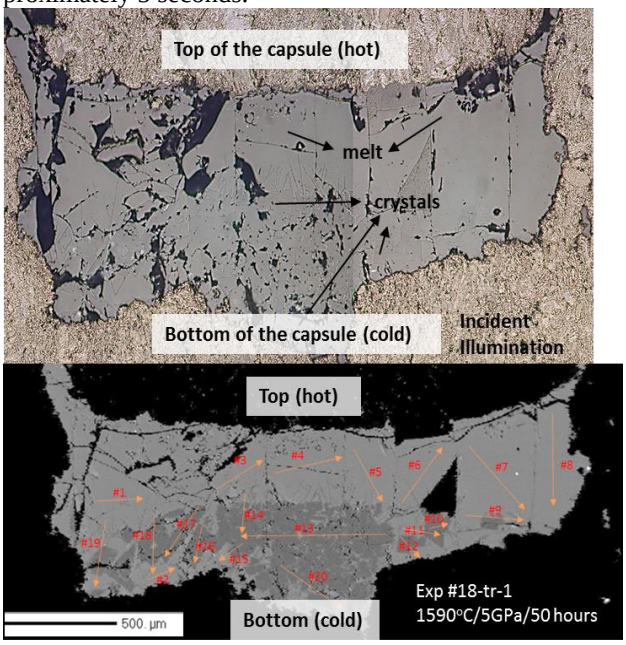

Fig. 2. Incident light (above) and back-scattered electron (BSE) image (below) of the section along the axis of the experiment. Notations on BSE image indicate EPMA analysis locations. Liquid is separating from the thermally compacted grossite crystals at the cold bottom of the graphite capsule.

Run products mounted in epoxy were sectioned, and polished for optical examination at LDEO and quantitative analysis using the Cameca SX100 electron microprobe (EPMA) at the American Museum of Natural History (AMNH). Trace element concentrations were determined using laser ablation ICP-MS at LDEO.

Preliminary Results: Composition #18 at 5 GPa and 1590°C achieved some thermal compaction: separation of homogeneous glass at the hot top part of the capsule and equilibrium grossite crystals with quench dendritic corners at the cold bottom (Fig. 2). Trace element concentrations in the glass were homogeneous. Initial melt trace element concentrations of 50 ppm were attained for all the trace elements except Sr. All the elements studied were found to be incompatible in grossite (Table 1). This was an expected result for HFSEs such as Zr, Nb, Hf, Ta, and Th. B's imcompatible behaviour in grossite, yet being a LILE, was interesting. Incompatibility of La, Ce, and Eu in grossite was suprising when compared to the published D values for hibonite ($^{\text{Hibonite-Melt}}$DLa: 4.9-7.2, $^{\text{Hibonite-Melt}}$DCe:3.9-5.2, and $^{\text{Hibonite-Melt}}$DEu: 2.8-3.5) [14]. The rest of the REEs incompatibility in grossite was similar to that of hibonite. These comprise the first trace element and REE partitioning data between grossite crystals and CAI-type liquids.

Table 1. Trace and REE composition of melt and grossite (ppm) determined with laser ICP-MS and calculated grossite–melt partition coefficients ($^{\text{Grossite–melt}}D$). Standard deviations were given in parentheses.

#18-tr-1	B	Sr	Zr	Nb	Ba	La	Ce
Glass (ppm)	38 (4)	130 (4)	45 (2)	50 (2)	75 (4)	66 (4)	62 (2)
Grossite (ppm)	1	41 (3)	0	3 (1)	7 (2)	6 (2)	7 (2)
$^{\text{Grossite–melt}}$D	0.03	0.31	0.01	0.06	0.1	0.09	0.12
#18-tr-1	Eu	Dy	Ho	Yb	Hf	Ta	Th
Glass (ppm)	57 (3)	45 (3)	43 (3)	43 (3)	37 (2)	41 (3)	40 (3)
Grossite (ppm)	7 (2)	3 (1)	3 (1)	2 (1)	1	2 (1)	1
$^{\text{Grossite–melt}}$D	0.13	0.07	0.06	0.05	0.03	0.04	0.04

Future Work: Systematic exploration of composition, temperature, and oxygen fugacity effects on trace and REE partitioning between phases such as melilite, olivine, and clinopyroxene and CAI-type liquids is in progress in several phase regions of Figure 1.

Acknowledgments: This research is supported by NASA Cosmochemistry grant NNX10AI42G (DSE) and the Kathryn Davis Postdoctoral Scholarship of the AMNH MAT program (GU).

References: [1] MacPherson G. J. (2004) In *Davis, A.M. (Ed.), Treatise on Geochemistry*, 201–246. [2] Boynton, W.V. (1975) Geochim. Cosmochim. Acta, 39**,** 56. [3] Grossman L. (1980) *Ann. Rev. Earth Planet. Sci. 8*, 559-608. [4] Stolper E. (1982) *Geochim. Cosmochim. Acta*, 46, 2159. [5] MacPherson G.J. et al. (1984) *J. Geol*., 92, 289. [6] Stolper E. and Paque J. M. (1986) *Geochim. Cosmochim*. Acta, 50, 1785. [7] Yoneda S. and Grossman L. (1995) *Geochim. Cosmochim. Acta 59*, 3413., 597-619. [8] Sweeney-Smith S.A. et al. (2010) *LPSC XLI*, Abstract #1877. [9] Nagasawa H. et al. (1980) *EPSL*, 46, 431-437. [10] Kuehner S.M. et al. (1989) *Geochim. Cosmochim. Acta*, 53, 3115–3130. [11] Beckett J.R. et al. (1990) *Geochim. Cosmochim*. Acta, 54, 1755–1774. [12] Lundstrom C.C. et al. (2006) *Geochim. Cosmochim. Acta*, 70, 3421–3435. [13] Ustunisik G. et al. (2014) *Geochim. Cosmochim. Acta*, 42, 27-38. [14] Ebel D. S. (2006) *MESS 2*, 253-277.